World Conference on Timber Engineering Oslo 2023

STUDY ON THE EVALUATION OF THE RESTORING FORCE CHARACTERISTICS OF FLOOR OF TRADITIONAL WOODEN BUILDING IN KYOTO

Rongji Fu[1], Mina Sugino[2], Yasuhiro Hayashi[3]

ABSTRACT: The vibration characteristics and seismic performance of traditional wooden buildings are heavily influenced by the restoring force characteristics of the floor. In this paper, we perform static loading tests on floors of traditional wooden buildings in Kyoto to understand the restoring force characteristics of floors of various specifications (Non-joist floor/ Joist floor). Then, Degrading Slip models (DS models) are used to develop highly accurate restoring force characteristics models of tested floors. In order to build restoring force characteristics models of floors with other specifications, a predictive formula for skeleton curves of floors is established. In addition, to calculate the skeleton curves of floors by using the formula, shear force-deformation models of a single nail are constructed by conducting the loading tests of floorboard-beam joints. The results indicated that 1) There are significant differences in restoring force characteristics of two different floors. 2) DS models can accurately represent the restoring force characteristics of the experiments. 3) Established predictive formula can simulate the skeleton curve of Non-joist floor with the shear force-deformation models of a single nail.

KEYWORDS: Traditional wooden building, Floor, Restoring force characteristics, Static loading test

1 INTRODUCTION

Since the 1995 Southern Hyogo Prefecture Earthquake, Japan has entered a period of seismic activity, and the risk of damaging earthquakes in various regions is increasing. And with the imminent occurrence of the giant Nankai Trough earthquake, inland crustal earthquakes are also said to occur frequently around that time. Meanwhile, there are many traditional wooden buildings in Japan. The promotion of seismic resistance reinforcement of these traditional wooden buildings is an urgent issue. Response obtained from time history response analysis can provide important information and basis for seismic resistance reinforcement.

To evaluate the response of the traditional wooden buildings against ground motions accurately, many static loading tests of structural components have been conducted to develop the analysis models. In this paper, we focused on the restoring force characteristics of floors, which affect the vibration characteristics of traditional wooden buildings.

The floors of Japanese traditional wooden buildings are usually consisted of wooden floorboards and steal nails. These floors have lower initial stiffness and bearing capacity than the floors of plywood is used due to sliding deformation between floorboards. But previous studies have shown that during large deformation angles, friction occurs between the floorboards, resulting in greater shear force [1-3]. Therefore, in this paper, we perform static loading tests on floors of traditional wooden buildings in Kyoto to understand the restoring force characteristics of floors of various specifications (Non-joist floor/ Joist floor) and to develop restoring force characteristics models. The models are aimed to describe the hysteresis characteristics with high accuracy to improve the accuracy of time history response analysis results. Then, to build restoring force characteristics models of floors with other specifications, a predictive formula for skeleton curves of floors is established. In addition, to calculate the skeleton curves of floors by using the formula, shear force-deformation models of a single nail are constructed by conducting the loading tests of floorboard-beam joints.

2 STATIC LOADING TEST

2.1 FLOOR SPECIMENS

The four specimens shown in Figure 1 and 2 are 1910 mm in the beam direction and 2865 mm in the girder direction, corresponding to half of a six-tatami room. The beams (270x120x2870 mm), girders (270x120x2910 mm), and small beams (180x120x1955 mm) of the specimens were all made of Oregon Pine (scientific name: *Pseudotsuga menziesii*). Dovetail joints were used to connect the beams and girders. Dovetail-dado joints were used between the girders and small beams. There were two types of non-joist floor specimens and joist floor specimens: those

[1] Rongji Fu, Kyoto University, Japan, rp-furongji @archi.kyoto-u.ac.jp
[2] Mina Sugino, Kyoto University, Japan, rp-sugino@archi.kyoto-u.ac.jp
[3] Yasuhiro Hayashi, National Institute Technology Maizuru Collage, Japan, y.hayashi@maizuru-ct.ac.jp

https://doi.org/10.52202/069179-0444

without floorboards (TS, TJ) and those with floorboards (FS, FJ). The floorboards of the Non-joist floor specimen FS were 30 mm thick cedar (scientific name: *Cryptomeria japonica*) boards, and two N90 (which means the length of the nail is 90 mm) nails were utilized to fix the floorboards to the beams. Joists (105x45x899 mm) were installed between each beam in joist floor specimens (TJ, FJ). Dado joints were used to connect joists and beams. And at the joint, the joist was fixed to the beam with N75 nails, one on each side. The joist floor specimen FJ was covered with 15 mm thick cedar boards, and floorboards were fixed to the beams with two N45 nails. The nailing interval for both specimens was 110 mm. Details of the floorboard-beam joint are shown in Figure 3.

2.2 LOADING METHOD

The loading system is depicted in Figure 4. The load was applied to the top of the specimens. To prevent the overall rotation of the specimens, a pantograph was used to keep the beam horizontal. The vertical displacement of the top beam of the specimens was not constrained. Two cycles of positive and negative alternating cyclic loading were used for the static loading test. The target displacement of the specimens took the deformation angle R = 1/450, 1/300, 1/150, 1/120, 1/100, 1/75, 1/50, 1/30, 1/20, 1/15, 1/10 and 0.15 rad. Figure 5 shows the specimen FJ under load.

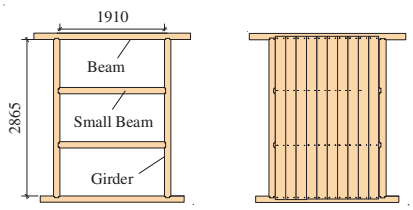

(a) *Specimen TS* (b) *Specimen FS*

Figure 1: *Non-joist floor specimens*

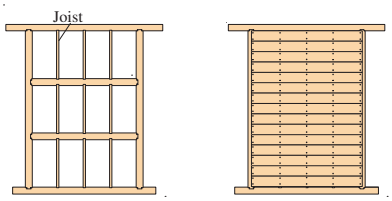

(a) *Specimen TJ* (b) *Specimen FJ*

Figure 2: *Joist floor specimens*

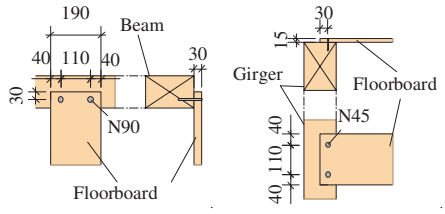

(a) *Specimen FS* (b) *Specimen FJ*

Figure 3: *Floorboard-beam joint*

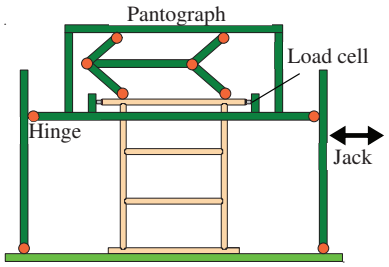

Figure 4: *Loading system of floor specimens*

Figure 5: *Specimen FJ under load (R = 0.15 rad)*

2.3 RESULTS

The restoring force characteristics of the floor specimens are shown in Figure 6. For all the specimens, the additional shear force due to the P-Δ effect was excluded using the method described in Ref [4].

At a target deformation angle R of 1/30 rad, the maximum load of TS and TJ was approximately 2 kN. Subsequently, as shown in Figure 7, the cracking of the dovetail joint developed, and the overall specimen load of the entire specimen decreased. Specimen TJ had slightly higher load at large deformation than Specimen TS due to the bending resistance of the joist.

For the Non-joist floor specimen FS, the load visibly increased about R = 1/15 rad. By R = 0.15 rad, no nail damage was observed.

Specimen FJ produced a shear force of 5.5 kN at 1/30 rad, and the load increased from 1/15 rad. The initial stiffness of specimen FJ was relatively high and the load gradually increased as the target deformation angle progressed. When the target deformation angle was small, the load at 0 rad was relatively high, but the load at 0 rad decreased with the applied load. During the large deformation, the nails of the upper and lower outer edge floorboards were pulled out from the girders as shown in Figure 8.

3 RESTORING FORCE CHARACTERISTICS MODELS

In this paper, the DS model developed by J.Nezaki et al. [5] was used to model the restoring force characteristics of the floor specimens. Degrading Slip model (DS model)

https://doi.org/10.52202/069179-0444

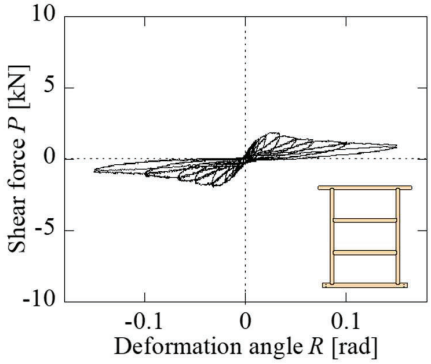

(a) *Specimen TS*

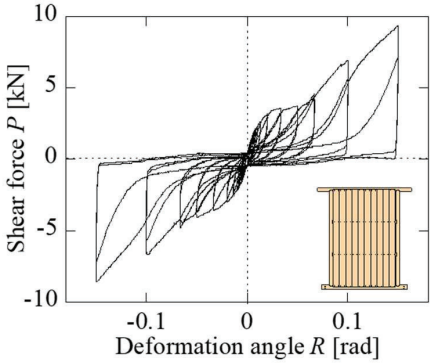

(b) *Specimen FS*

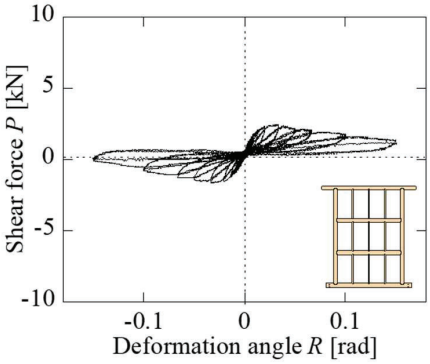

(c) *Specimen TJ*

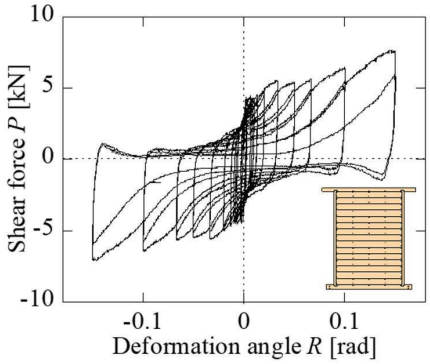

(d) *Specimen FJ*

Figure 6: *Restoring force characteristics*

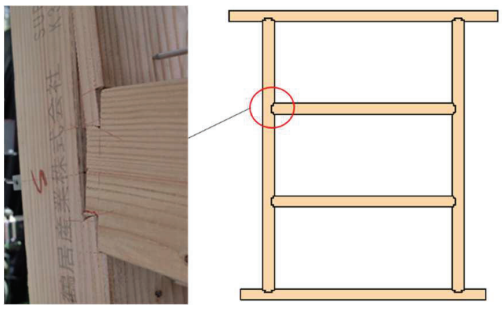

Figure 7: *The crack of the dovetail joint*

Figure 8: *Pulled out nail*

can describe the lowering slip stiffness around zero deformation angle as the maximum experienced deformation angle increases.

Figure 9 shows a comparison between the experimental data with the DS models. The figure illustrates that the DS models accurately represented the restoring force characteristics of the experiments. The initial stiffness of the TS, TJ specimens differed insignificantly. When the boards were applied, the initial stiffness of the Non-Joist floor increased by a factor of two, while that of the joist floor increased by a factor of eight. Furthermore, for specimen TS and FS the shear force Q_0 at the deformation angle of 0 rad of the hysteresis loop was 0.2-0.4 kN, which was not much different between the two specimens. While the shear force Q_0 at the deformation angle of 0 rad of FJ was much higher than Q_0 of TJ. Therefore, the area of the hysteresis loop of specimen FJ was larger than that of the TJ.

4 MECHANICAL MODEL

In Chapter 3, the restoring force characteristics models of the floor specimens were built. However, in actual traditional wooden buildings, the results obtained from experiments cannot be used directly in design because the specifications vary widely from building to building. Since the parameters of the DS models are mostly decided

https://doi.org/10.52202/069179-0444

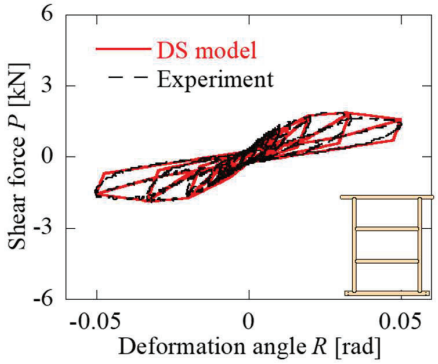

(a) *Specimen TS*

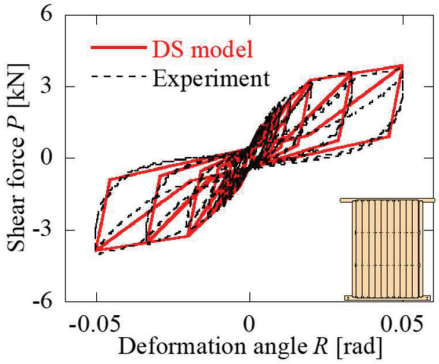

(b) *Specimen FS*

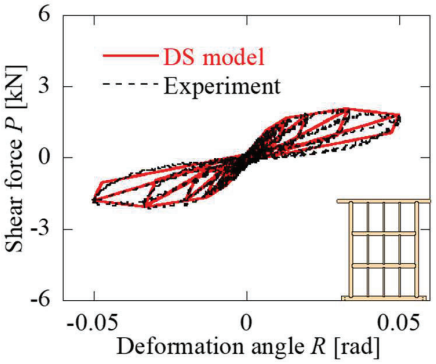

(c) Specimen TJ

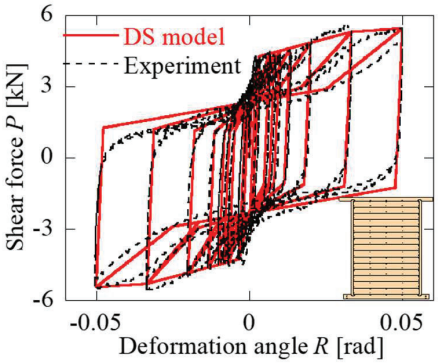

(d) *Specimen FJ*

Figure 9: *Restoring force characteristics models*

according to the skeleton curve of floors, it is necessary to estimate the skeleton curve in developing restoring force characteristics models for floors with varying specifications, such as the number of nails and floorboard orientation. In this chapter, we started by building a shear force-deformation models for a single nail joint. The shear force-deformation models were then used to create a prediction formula that can simulate the skeleton curve of the entire floor.

4.1 SHEAR FORCE-DEFORMATION MODELS OF NAIL JOINT

Figure 10 shows the specimens simulating the floorboard-beam joint. At the floorboard-beam joint, the boards' movement causes the nails to bend in the same direction. The direction of movement of the boards is random because of the seismic load. Therefore, the effect of the direction of movement of the board on the nails' resistance characteristics needs to be confirmed by experimentation. As shown in Figure 10, there were 3 types (PV, PP, VP) of floorboard-beam joint. The fiber orientations of the floorboard and beam were different for each of the 3 types of floorboard-beam joint. To correspond to the floor specimens FS and FJ described in the Chapter 2, each type of floorboard-beam joint had two specimens with the same length of nails (N45 and N90) and thickness of the floorboard (15 mm and 30 mm) as specimens FS and FJ.

The loading systems are shown in Figure 11. The beam was fixed and positive and negative cyclic forces were applied to the floorboard side. The target displacement δ of the nails were 1, 2, 4, 6, 8, 10, 15, 20, 25 mm.

The skeleton curves of shear force-deformation characteristics of a single nail are shown in Figure 12. The figure shows that the maximum load of the single N90 nail in PV specimen was about 15% lower than that of the single nail of other specimens. On the other hand, the single N45 nail in PV specimen had a higher maximum load than the single nail in the other specimens. The differences between specimens with nails of the same length were likely due to specimen variability rather than fiber direction effects. Since no significant fiber direction effects were identified, the average of the results from the three types of specimens was used to model the shear force-deformation relationship for a single nail. The results are shown in Figure 13.

4.2 PREDICTIVE FORMULA FOR SKELETON CURVES

In the formula, the floor shear force was divided into three sections: the shear force of the floor frame P_b; the shear force P_n caused by nails; and the shear force P_f due to friction. The skeleton curve of the DS model of the TS, TJ specimens were used to represent the floor frame shear force P_b. The force P_n and P_f were calculated by the formula suggested in Ref [3]. Taking the specimen FJ as an example, the formula is explained as follows.

https://doi.org/10.52202/069179-0444

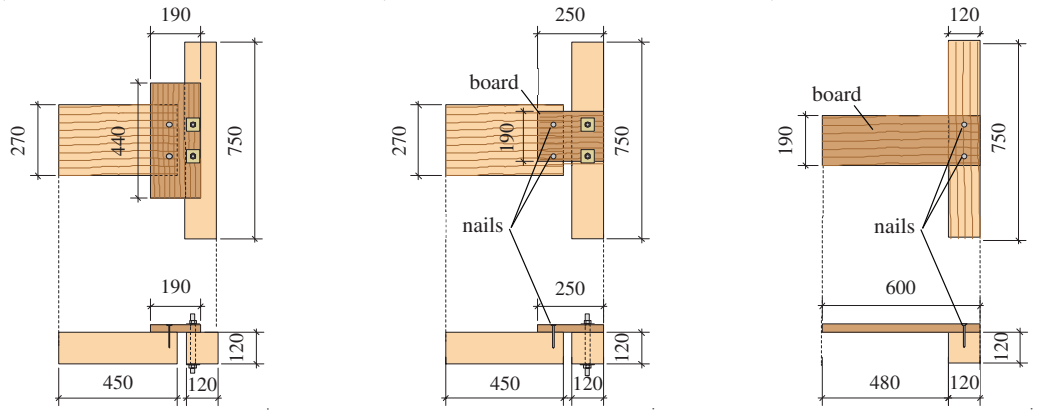

(a) *Specimen PV* (b) *Specimen PP* (c) *Specimen VP*

Figure 10: *Floorboard-beam joint type*

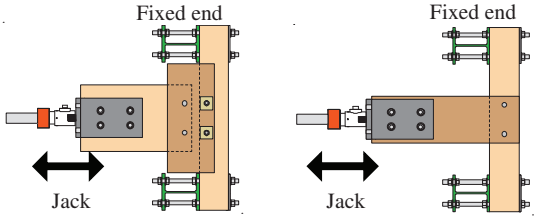

(a) *PV, PP* (b) *VP*

Figure 11: *Loading systems of joint specimens*

The height of floor specimens is H, the deformation angle is R and the number of floorboards is N. As shown in Figure 15 the deformation caused by the rotation of the floorboards δ_x is calculated from Equation (1). When the rotation angle of the specimen occurs, the height of the specimen will shrink relative to the height of all the floorboards. The amount of shrinkage must be symmetrically distributed from the centre of the specimen. Therefore, as shown in Figure 14, when the centre of the girder is considered as the centre of rotation, the shrinkage $\delta_y(i)$ corresponding to the distance $h(i)$ from the centre of

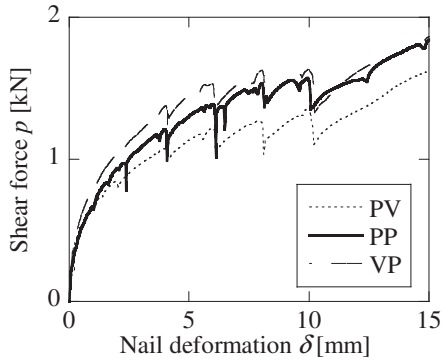

(a) *N90 nail*

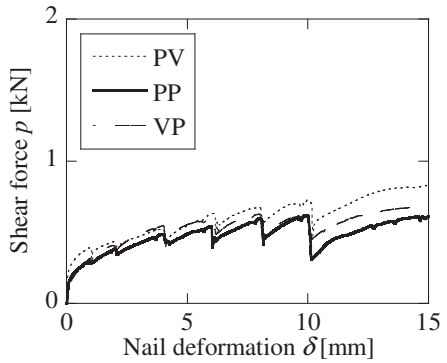

(b) *N45 nail*

Figure 12: *The skeleton curves for a single nail*

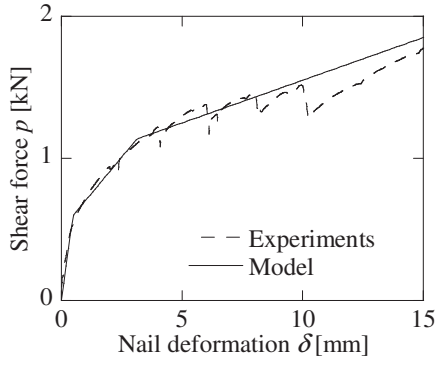

(a) *N90 nail*

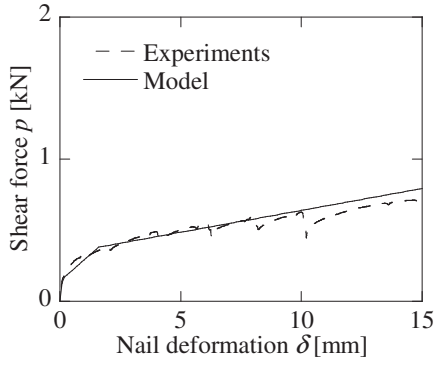

(b) *N45 nail*

Figure 13: *The shear force-deformation relationship for a single nail*

https://doi.org/10.52202/069179-0444

each floorboard to the centre of the specimen can be calculated from Equation (2). The symbol (*i*) represents the *i*-th board. The shrinkage $\delta_y(i)$ can be seen as the y-axis deformation of nails in the i-th floorboard. So, the total deformation δ can be calculated from Equation (3). Substituting the total deformation δ of the nail (*i*) into the nail shear force-deformation relationship constructed in Chapter 4.1, the total shear force of the nail $p_{45}(i)$ can be obtained. The x-axis and y-axis shear force $p_x(i)$ and $p_y(i)$ can be calculated from Equation (4) as shown in Figure 16. Then, the resistance moment M_n of the whole specimen can be obtained from Equation (5). Here, *m* is the number of nail joints per board (*m* = 5 for joist floor specimen FJ). The friction force between the boards is then calculated from the y-component $p_y(i)$ (Equation (4)) and the coefficient of friction. The frictional force $p_f(i)$ acting on the *i*-th plate, as shown in Figure 17, can be obtained from the difference between the upper and lower plate frictional forces from Equation (6). The resisting moment M_f can be obtained from the frictional force $p_f(i)$ and the distance $h(i)$ from the centre of the floor specimen (Equation (7)). The resisting moments M_n and M_f divided by the height of specimen *H* are the resisting forces P_n and P_f (Equation (8)).

The simulation results for a friction coefficient μ of 0.3 are shown in Figure 18. The shear force P_b of the floor frame was the skeleton curve of the restoring force characteristics model of the floor flame specimen TS and TJ built in Chapter 3; the shear force $P_{(model)}$ of the floor specimen was calculated by adding P_b, P_n and P_f.

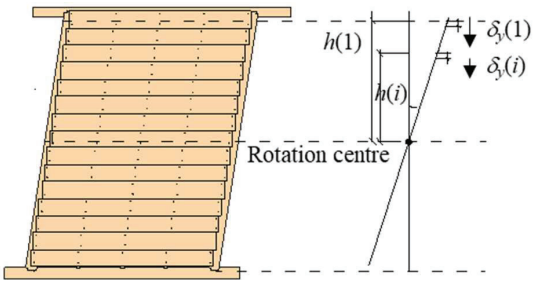

Figure 14: *y-axis deformation*

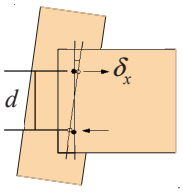

Figure 15: *x-axis deformation*

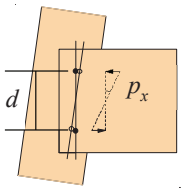

Figure 16: *x-axis force*

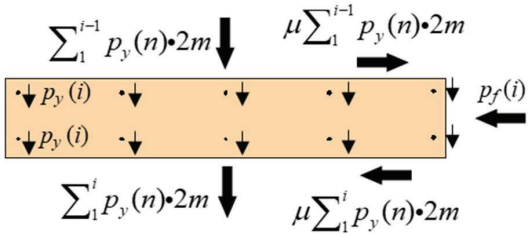

Figure 17: *Friction force caused by y-axis force $p_y(i)$*

$$\delta_x = \frac{d}{2}\sin R \tag{1}$$

$$\delta_y(i) = h(i)\ (1-\cos R) \tag{2}$$

$$\delta(i) = \sqrt{(\delta_y(i))^2 + (\delta_x)^2} \tag{3}$$

$$p_x(i) = p_{45}(i)\ \frac{\delta_x}{\delta(i)} \quad p_y(i) = p_{45}(i)\ \frac{\delta_y(i)}{\delta(i)} \tag{4}$$

$$M_n = m\ \sum_{i=1}^{N} p_x(i)\ \frac{d}{2} \tag{5}$$

$$p_f(i) = 2m \cdot p_y(i)\ \mu \tag{6}$$

$$M_f = \sum_{i=1}^{N} p_f(i)\ h(i) \tag{7}$$

$$P_n = M_n / H \qquad P_f = M_f / H \tag{8}$$

The shear force $P_{(exp)}$ was the skeleton curve of the restoring force characteristics model built in Chapter 3. The figure shows that $P_{(model)}$ and $P_{(exp)}$ of the FS specimen corresponded approximately. The load was carried by the floor flame during micro-deformation. The frictional force P_f increased gradually with increasing deformation angle. From *R* = 1/30 rad, the shear force of the floor flame decreased due to cracks in the dovetail joints, so the shear force of the floor specimens was borne by the nails and frictional forces.

On the other hand, for the specimen FJ, the difference between the model and the experimental result for the initial stiffness was significant. Predictive formula for skeleton curves of Joist floor should take further consideration.

5 CONCLUSIONS

In this research, we have used static loading tests on traditional wooden buildings floors to develop highly accurate models of restoring force characteristics for two types of floors. In addition, the shear force-deformation models of a single nail has been used to build a mechanical model that can estimate the skeleton curve of the floor. The results indicated that

1) There are significant differences in restoring force characteristics of two different floors.
2) DS models can accurately represent the restoring force characteristics of the experiments.
3) Established predictive formula can simulate the skeleton curve of Non-joist floor with the shear force-deformation models of a single nail.

ACKNOWLEDGEMENT

The authors would like to thank Y. Kimoto for his assistance through this research. This research is supported by JSPS Grants-in-Aid for Scientific Research JP19H00793. Part of this work was supported by JST SPRING, Grant Number JPMJSP2110.

https://doi.org/10.52202/069179-0444

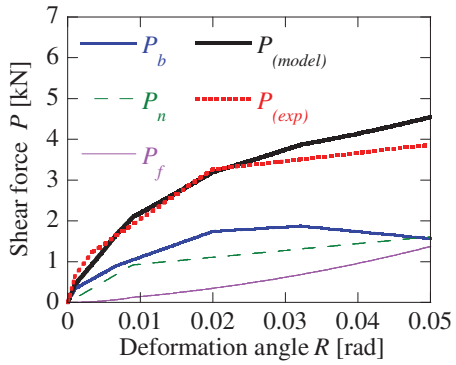

(a) *Specimen FS*

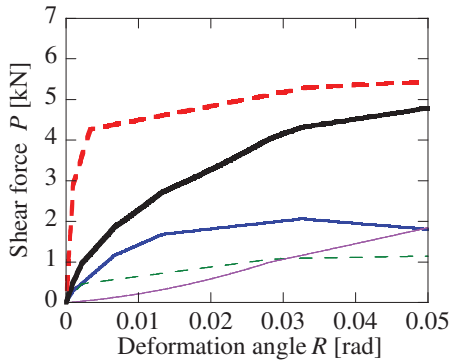

(b) *Specimen FJ*

Figure 18: *Simulation results for a friction coefficient μ of 0.3*

REFERENCES

[1] T. Kamada and D. Fukumori: Bearing Characteristics for Shearing Deformation of Floor Systems of Traditional Wooden Houses. Bulletin of Faculty of Engineering, Fukuyama University, 31:131-138, 2007. (in Japanese)

[2] M. Minami, A. Kitamori, K. Jung and K.Komatsu: Shear Peformances of the Floor System Using Japanese Cedar Planks. Japan's Journal of Structural and Construction Engineering, Vol.74, No.644:1785-1793, 2009. (in Japanese)

[3] A.Takino, Y.Azumi, S.Okamoto, T. Nakagawa, T.Shibutani and M.Murakami: Formula to Predict the Shear Peformance of Floor Construction of Traditional Wooden Structures Considering the Increasing Strength Based on Friction. Japan's Journal of Structural and Construction Engineering, Vol.79, No.703:1329-1336, 2014. (in Japanese)

[4] T.Morii, M.Miyamoto, H.Takahashi and Y.Hayashi, Influence of P-Δ Effects on Deformation Capacity of Wooden Frames Structure. Japan's Journal of Structural and Construction Engineering, Vol.75, No.650:849-857, 2010. (in Japanese)

[5] J.Nezaki, R.Fu, M.Sugino, and Y. Hayashi: Modeling and Respond Analysis of Resilience Characteristics of Traditional Japanese Wooden Frame structure with Earthen Walls Part 1: Modeling Methods for Resilience Characterics. In: Annual Conference Proceedings of the Architectural Institute of Japan, Structure II, 261-262, 2022. (in Japanese)